

## The Effects of Gas Tungsten Arch Welding on the Corrosion and Mechanical Properties of AA 6061 T6

Elsadig. Eltai\*, E. Mahdi, Akram Alfantazi

Qatar University, Department of Mechanical and Industrial Engineering, P.O. Box 2713, Doha, Qatar.

\*E-mail: [elsadigms@qu.edu.qa](mailto:elsadigms@qu.edu.qa)

Received: 10 March 2013 / Accepted: 4 April 2013 / Published: 1 May 2013

---

Corrosion of welded and un-welded Aluminum Alloy 6061 T6 was investigated by immersing specimens in 3.5% (wt) NaCl solution. Potentiodynamic and open circuit potential measurements were conducted. The mechanical properties were investigated using tensile strength, hardness, and torsion tests. Optical Microscopy and Scanning Electron Microscopy were used to investigate the microstructure evolution and the failure pattern of the specimens. Results revealed that corrosion current of the heat affected zone (HAZ) was higher than the base metal (BM). Corrosion potential for HAZ was more negative than the BM. Significant pitting corrosion was observed on the HAZ compared to the BM. Welding was found to weaken the mechanical properties of the alloy. Welded tensile specimens were failed at the welded area whereas not welded ones were failed at the centre. Welded torsion specimens were failed at the HAZ but not welded ones failed at the centre. The hardness of HAZ was decreased as a result of the heat generated during the welding process. Hardness values were increased as we moved away from the welded region.

---

**Keywords:** Welding, HAZ, Corrosion, Mechanical properties, BM

### 1. INTRODUCTION

Aluminum and Aluminum alloys are used extensively in different industries such as structural and transportation, etc.. The reasons behind that are many, good mechanical properties, acceptable corrosion resistance, light weight, high strength, appropriate weldability, and high toughness [1]. Recently, AA has become very attractive materials for scientist and engineers and has been studied extensively due to its good properties. However, more studies need to be carried out in order to improve the properties of AA comparing to steel, it is expected that substitution of AA for steel will result in big improvements in energy economy and recycling. Welding of Aluminum alloys is a critical operation due to the complexity and the high level of defects that may occur during the welding

process because Al and its alloys are well known that they are highly reactive with oxygen, they have high thermal conductivity, and they have high hydrogen solubility at high temperature [2-4].

Tungsten Gas Arch Welding (TIG) is one of the most important welding processes; it uses a non-consumable tungsten electrode to produce the weld. TIG is widely used to weld Al-Mg alloys [5]. The initial strength of non-treatable Aluminum alloys depends on the hardening effect of the different elements that available in the alloy such as silicon, magnesium, manganese, and iron [6]. The mechanism by which these elements increase the strength is through dispersed phase or by solid solution strengthening. Vaporization of alloying elements may take place during the welding process which may influence the mechanical properties of the welded areas by affecting the chemistry of the weld pool [7]. The effect of arc oscillation in either transverse or longitudinal direction is very beneficial to the fusion zone microstructure and tends to reduce sensitivity in hot cracking [8,9]. Aluminum alloys will remain the subject of extensive studies due to their susceptibility to localised corrosion in different corrosive environments especially in chloride containing environment, in such corrosion environment Aluminum alloys tend to show pitting corrosion and stress corrosion cracking [10,11].

The purpose of this research is to study the corrosion behavior of the Heat affected zone (HAZ) compared to Base Metal (BM) of Al alloy 6061 T6 using immersion test, Scanning Electron Microscopy, and Optical Microscopy. The effects of welding on the mechanical properties of the alloy have also been investigated using tensile, hardness, and torsion tests.

## 2. EXPERIMENTAL PROCEDURE

### 2.1 Corrosion test

The material used in this study was Aluminum alloy 6061 T6. The composition of the alloy is shown on table 1. Cylindrical shaped metallic specimens were prepared using a cutting machine; the material was cut into small pieces. Each specimen was embedded in an epoxy with an exposed surface of 0.28 cm<sup>2</sup>. A corrosion environment consisting of 3.5% (wt) NaCl in distilled water was prepared. To remove any grease or impurities that may present on the specimens, they were washed with soapy water and ethanol. Specimens were then dried with hot air stream before being immersed in the solution. Experiments were conducted at room temperature which is approximately (20±1°C).

**Table 1.** Chemical composition of Al alloy 6061 T6

Metal	Al	Si	Mg	Cu	Cr	Mn	Zn	Ti	Fe
(Wt%)	95.8-	0.4-	0.8-	0.15-	0.04-	Max	Max	Max	Max
	98.6	0.8	1.2	0.4	0.35	0.15	0.25	0.15	0.7

To compare the corrosion behavior of the heat affected zone (HAZ) and the base metal (BM), corrosion potential and potentiodynamic polarisation were evaluated independently by separating these

zones from the weld joint, tests were carried out using Gamry potentiostat DC105 manufactured by Gamry instruments, USA. The scan rate was 1.00 mV/s. Samples were then put in a cell containing the NaCl solution that was prepared. Corrosion potential was monitored over a period of 4 hours. A three electrode cell was used, the three electrodes being the specimens as working electrode, saturated calomel as reference electrode, and a graphite counter electrode. .

## 2.2 Mechanical tests

The gas tungsten arch welding (TIG) method was used to weld the specimens. To conduct the welding process, welding machine with capability of changing its electric current was used. Specimens were welded under Ar (99% purity) atmosphere and a current of 110 Ampere using Miller Syncrowave 350 LX machine manufactured in the USA. The type of filler used for the welding process was AlMg5 alloy wire; the composition of the alloy is presented in table 2. To remove any contaminants (oil, grease etc..) that may present as a result of the cutting or handling process, the work pieces were wiped with ethanol before being welded.

**Table 2.** Chemical composition of AlMg5 alloy

Metal	Si	Mg	Mn	Al
Wt %	0.2	5	0.05- 2	Balance

Specimens for tensile testing were machined to ASTM E8-04 standards. A CNC milling machine was used to cut the specimens into the specified dimension. Tensile test was conducted using a computer controlled testing machine (Instron, Model 5585H manufactured in USA) with a capacity of 250 KN and a cross head speed of 5 mm/min.

Rockwell hardness test was made as per ASTM E18-05 standard. Hardness test was carried out on circular welded samples with a load of 60 kg, a ball indenter of 1/16 inch diameter, and duration of 15s using Indentec hardness tester Model 8187.LKV. UK. Four different readings were taken around the welded circular area; the same number of readings was then taken at an interval of 5mm away from the welded area longitudinally.

Specimens for torsion test were prepared as per ASTM E143-87 standard. Test was carried on welded and un-welded specimens using a computer controlled machine (Jinan testing machine, model NDW-2000 manufactured in China) with a rotation speed of 90°/min.

## 2.3 Microstructural observation

Microstructural observation for HAZ and BM was conducted using scanning electron microscopy (SEM). The same techniques were also used to investigate the failure pattern for tensile and torsion specimens after failure.

### 3. RESULTS AND DISCUSSION

The electrochemical corrosion behavior of HAZ and base metal (BM) was evaluated independently by separating these zones from each other, and then it was exposed to 3.5% NaCl solution. Fig1 shows typical potentiodynamic polarisation plots for HAZ and BM. As can be seen, the base metal has a corrosion potential of -718mv, and a corrosion current of 0.3  $\mu$ A. The corrosion potential of HAZ was -1,24 V and the corrosion current was 0.9 $\mu$ A. Fig 1 indicated that the corrosion resistance of HAZ was less than the base metal. Important information can be derived from fig 1 regarding pitting corrosion, it is apparent that pitting at HAZ was severely occurred compared to the base metal, the possible interpretation for that is the heat that generated during the welding process which caused thermal alterations and negatively affected the corrosion resistance of the alloy [4]. This result was supported by images obtained for HAZ and BM after immersion (figs 3 and 4). In addition to that, the formation of dendritic structure with heterogeneous concentration distribution may cause poor corrosion performance [12-13].

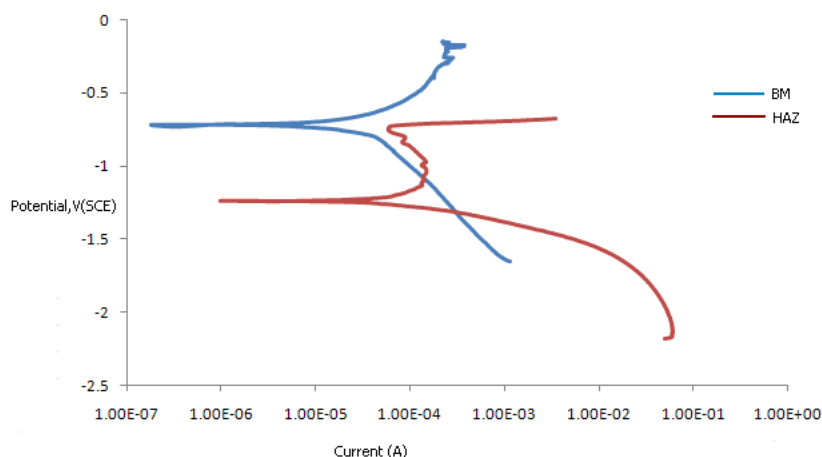


**Figure 1.** Potentiodynamic polarisation for HAZ and BM in 3.5% NaCl solution

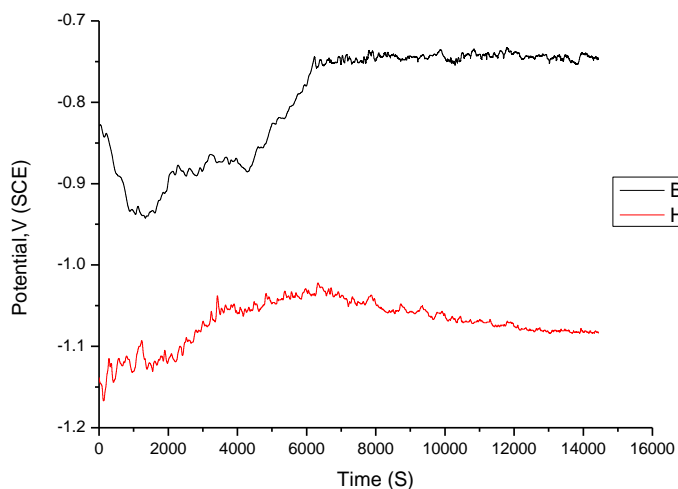


**Figure 2.** Time dependent of corrosion potential for HAZ and BM

The OCP values of HAZ and BM after exposure to the test solution for 4 hours are presented in fig 2. It is apparent that the OCP values of HAZ were more negative than the ones for BM. This may be interpreted as poor corrosion resistant. It is also apparent that OCP of HAZ was fluctuated with many positive and negative peaks suggesting the occurrence of pitting corrosion on the specimens; this result was supported by the observation of severe pitting corrosion on the exposed surface (fig 4).

The different between the two potentials certificates the formation of a galvanic cell. Such potential differences caused the formation of corrosion cells. As the percentage of these cells increases; the resistance of the alloy to corrosion will decrease.

Fig 3 (a-b) shows images of the BM surface after potentiodynamic polarisation, it is obvious that pitting corrosion has occurred on the surface as a result of being exposed to the corrosive media.

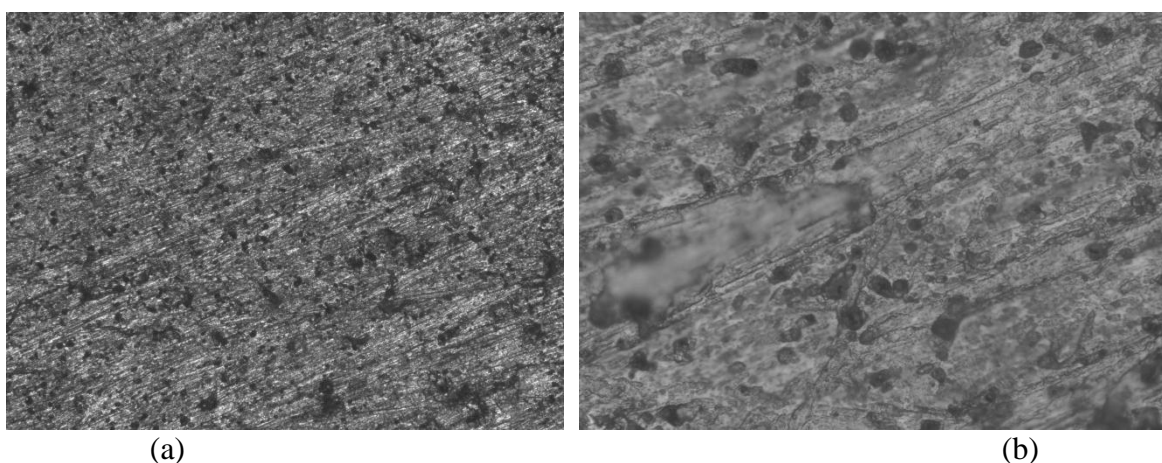


**Figure 3.** Optical Microscope of corrosion surface of BM after potentiodynamic test: (a) at low magnification (100X) and (b) at high magnification (500X)

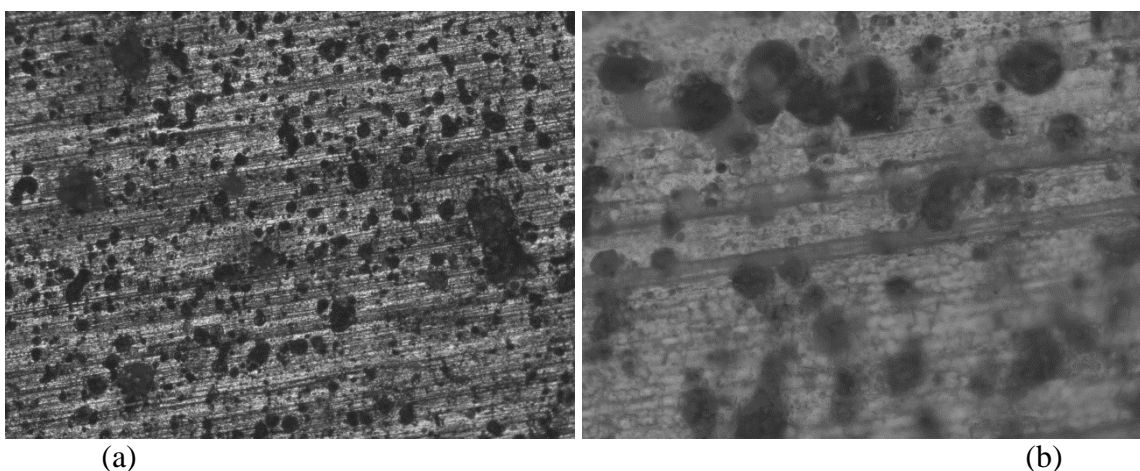


**Figure 4.** Optical Microscope of corrosion surface of HAZ after potentiodynamic test: (a) at low magnification (100X) and (b) at high magnification (500X)

In the case of HAZ as per fig 4, severe pitting and intergranular corrosion has taken place. However, the diameter of the pits was bigger than the BM which can be attributed to the exposure of this part of the specimens to high temperature during the welding process which caused modification in microchemistry and microstructure of the HAZ. Consequently, this region has a poor corrosion resistance when compared to BM [4,14].

Based on fig 5, it is obvious that the surface was severely corroded indicating that the HAZ exhibits the highest susceptibility to intergranular corrosion as well as localised corrosion. Coarse precipitates and deep pits can be clearly seen on the surface. Rhodes et al [14] were found that Localised corrosion of Al initiates as pitting corrosion and then propagates to intergranular corrosion.

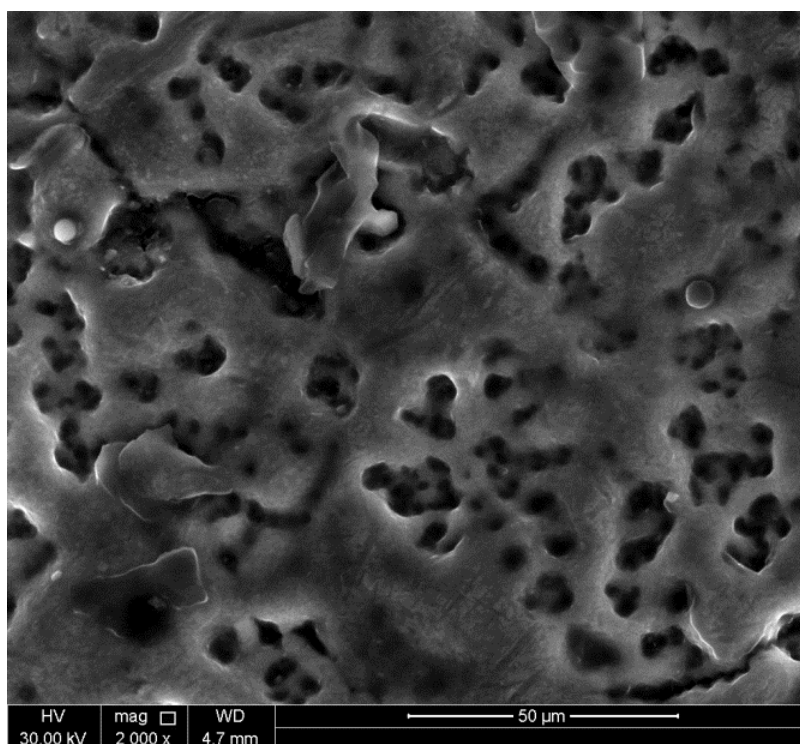


**Figure 5.** Coarse grain boundary and intergranular precipitates in the HAZ of AA 6061 T6

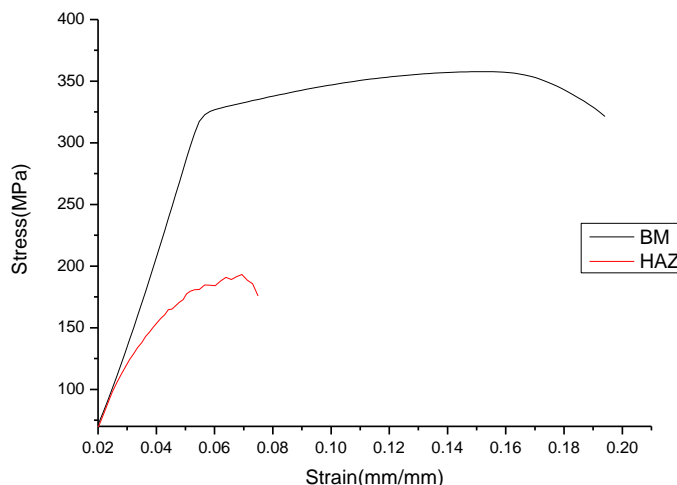
Un-welded specimen for tensile test was broken at the centre of the specimen. However, welded one was broken at the welded area (figs 9, and 11) suggesting that the welded region is the weakest part of the specimen, the softening in such area was attributed to a loss of strain hardening associated with fusion during the TIG welding process [15]

Fig 6 shows stress vs strain plot for welded and un-welded specimen, it is apparent that the ultimate tensile strength (UTS) for welded specimen was less than the un-welded one by almost 46%. Resulting yield stress (YS), Fracture stress, elongation percent, and reduction in Area percent were calculated and presented in table 3. It is apparent that the welded specimens have limited elongation capability compared to the un-welded ones because the total elongation of the specimens during tensile

test was concentrated in the HAZ which is obviously the weakest zone as it was shown in the current study.

**Table 3.** Tensile properties for welded and un-welded specimens

Tensile property	Ultimate tensile strength (MPa)	Yield stress (MPa)	Fracture stress (MPa)	Elongation (%)	Reduction in area (%)
Welded specimen	193.107	146.438	175.81	7.4	7.4
Un-welded specimen	357.747	322.75	321.373	12.1	32.9



**Figure 6.** Stress vs Strain plot for welded and un-welded specimens

Table 4 shows values of hardness at the welded area and at different location away from the welded area. Considerable variation in the hardness values was observed.

**Table 4.** Hardness values for welded specimen

Distance (mm) from the weld	0	5	10	15	20
Hardness value (HRF)	38.02	23.4	52.4	70.5	81.6

Table 4 and fig 7 demonstrate that the minimum hardness value was recorded at a distance of 5 mm away from the weld. The highest hardness value was 81.6 HRF at a distance of 20mm away from the weld. Fig 7 shows the hardness profile for welded area and at different distances away from the weld. As presented, the hardness values were increased as we moved away from the weld region

suggesting that the HAZ has a lower plastic deformation capability than the rest of the base metal, softening of HAZ can be attributed to the dissolution of strengthening  $\beta''$  ( $Mg_2Si$ ) precipitate[16]. The portion of the HAZ close to the weld is harder than the rest of the HAZ but still softer than the base metal.

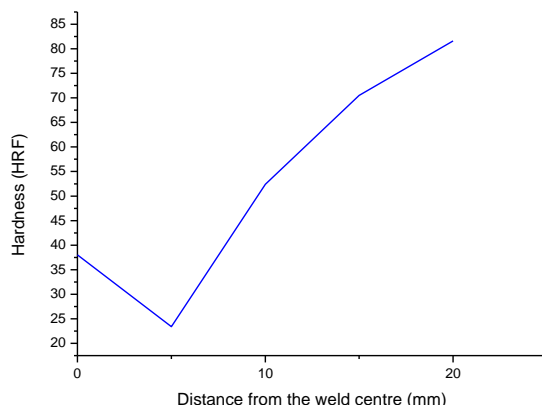


**Figure 7.** Hardness profile for welded area and away from the weld

Fig 8 displays torque vs angle curve for welded and un-welded specimens, it is obvious that the magnitude of torque for un-welded specimens is higher than the welded ones suggesting that the TIG welding has an influence on the torsion strength of the alloy. The torsion test demonstrates that the un-welded specimens broke in the middle whereas, the welded ones broke at the HAZ due to overheating of this area (fig 11), so grain growth was promoted by the absorbed heat [17], consequently, coarse grains was developed in the HAZ, these coarse grains caused a decrease in the mechanical properties of the welded specimen as proved by the torsion and corrosion tests in this study. It is clear from this that, the welded area of Al alloy 6061 T6 becomes harder than the HAZ and the fracture therefore occurs in the heat affected zone. This result was in agreement with the hardness test that conducted which proved that the welded area has a higher hardness value compared to the HAZ (Table 3 and fig 7).

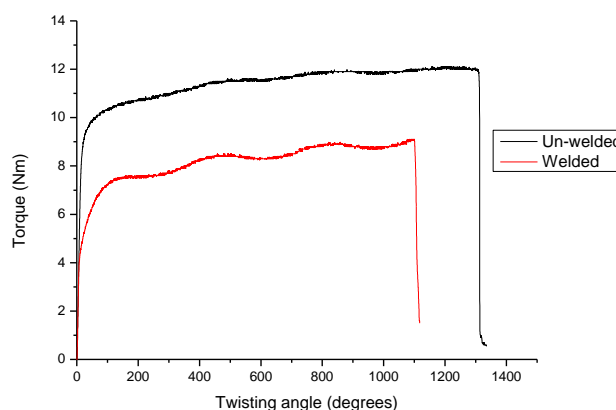


**Figure 8.** Torque vs Angle for welded and un-welded specimens

*Fracture analysis*

The visual inspection of the rupture surface after tensile test revealed two types fracture topography 90° type and V type. The 90° type fracture surface was the dominant type for welded specimens. The V type was the dominant type for the un-welded specimens. The welded tensile specimen broke at the welded region suggesting that this region is the weakest part of the specimen (fig 9a). The un-welded specimen was broken at the centre (fig 9b).

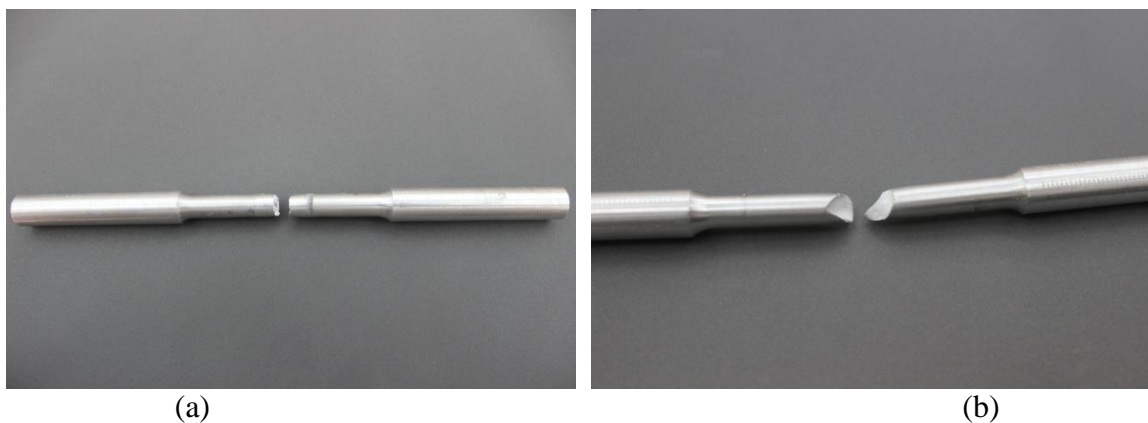


**Figure 9.** Positions of failure for welded specimens (a) welded, and (b) un-welded during tensile test

Welding process of Al and Al alloy represents a great challenge; care needs to be taken while conducting the process, one of the drawbacks of Al welding is the presence of defects in the welded area. Such defects may affect the mechanical and corrosion properties of the welded material. The properties of Al and Al alloys such as high thermal conductivity and high chemical reactivity with oxygen contributes to the presence of defects and voids during the welding process. In order to understand the fracture pattern of welded and un-welded AA 6061 T6 specimens, the fracture surfaces of the tensile specimens were characterised using SEM technique. Micrographs were taken at different areas and presented in fig 10a and 10b. Fig 10a shows fracture surface of welded specimen which shows feature of ductile fracture, in addition to that, the size and the spacing between the grain produced at welded area were big which is an indicative of the ductility of the welded area, the grains were large and the distance between them was big. Based on fig 10a, it can be observed that dimples dominated the fracture surfaces reflecting the fact that most of the failure was the result of the ductile fracture, this interpretation was in agreement with the work that done by many authors [18,19]. In the case of non-welded specimen as in fig 10b, the grain size was small and the distance between different grains was also small. Fig 10b clearly reveals feature of brittle fracture and elongated white fibrous tips due to the stress that being applied.

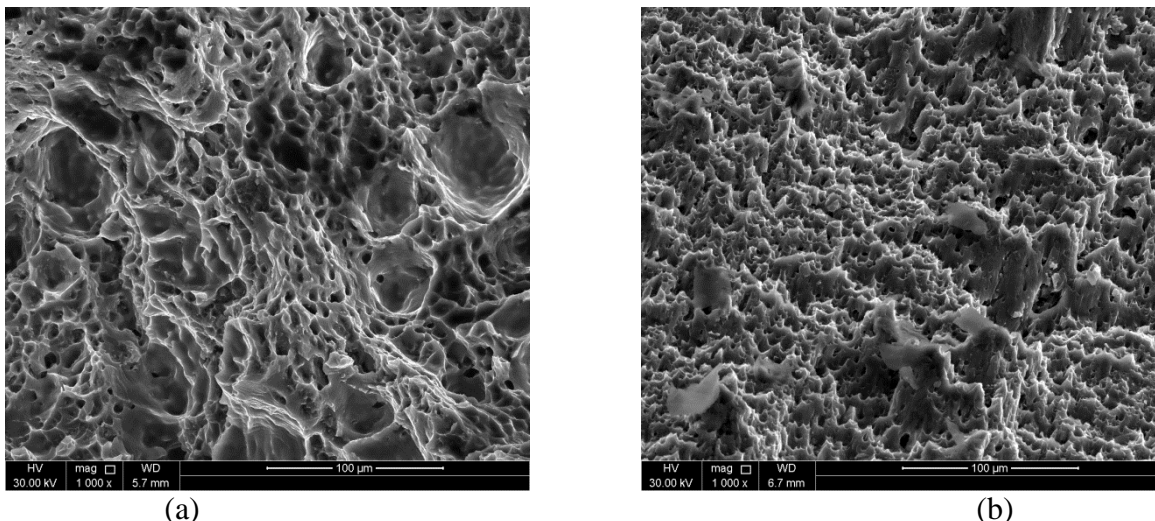


**Figure 10.** SEM micrographs of failed tensile specimens, (a) welded, (b) un-welded (b)

In torsion test, the welded specimen broke at the HAZ (fig 11a) suggesting that the heat generated from the welding process affected the mechanical properties of this area, this result was in agreement with the corrosion test that conducted for the HAZ as it was found that the HAZ was more susceptible to corrosion because of the heat input during welding. The non welded specimen broke at the middle (fig 11 b).

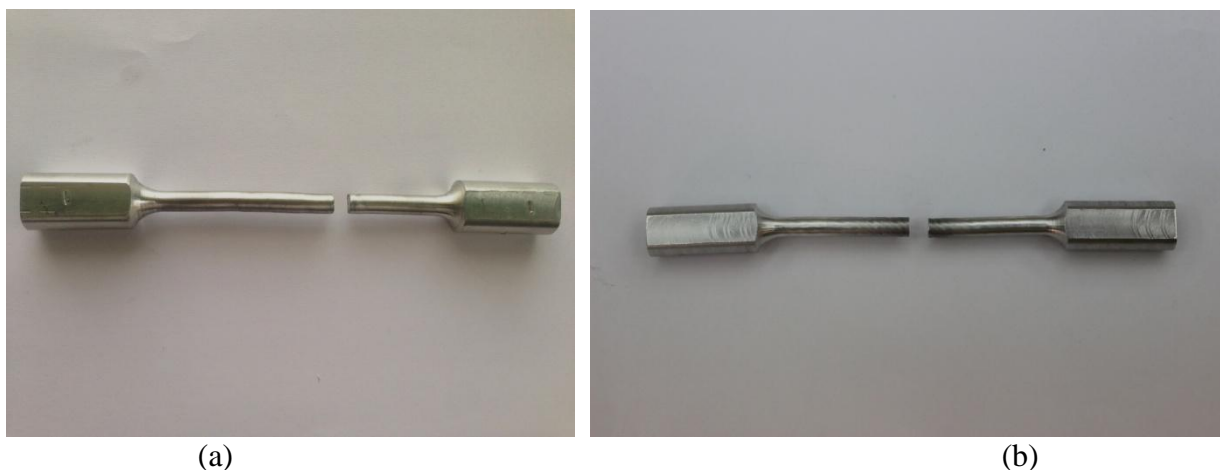


**Figure 11.** Positions of failure for specimens (a) welded, and (b) un-welded after torsion test

Figs 12a and 12b compares the SEM micrographs of the fractured area for welded and un-welded specimens after torsion test. As mentioned earlier the welded specimens were failed at the HAZ. It is obvious that at this zone, large void particles are visible, In addition to that, the microstructure is inhomogeneous and coarse due to the welding process [20]; therefore a weak area was formed at the HAZ causing the specimen to fail [21-24]. The microstructure for the un-welded specimen after torsion test is fine with small voids (fig 12b)

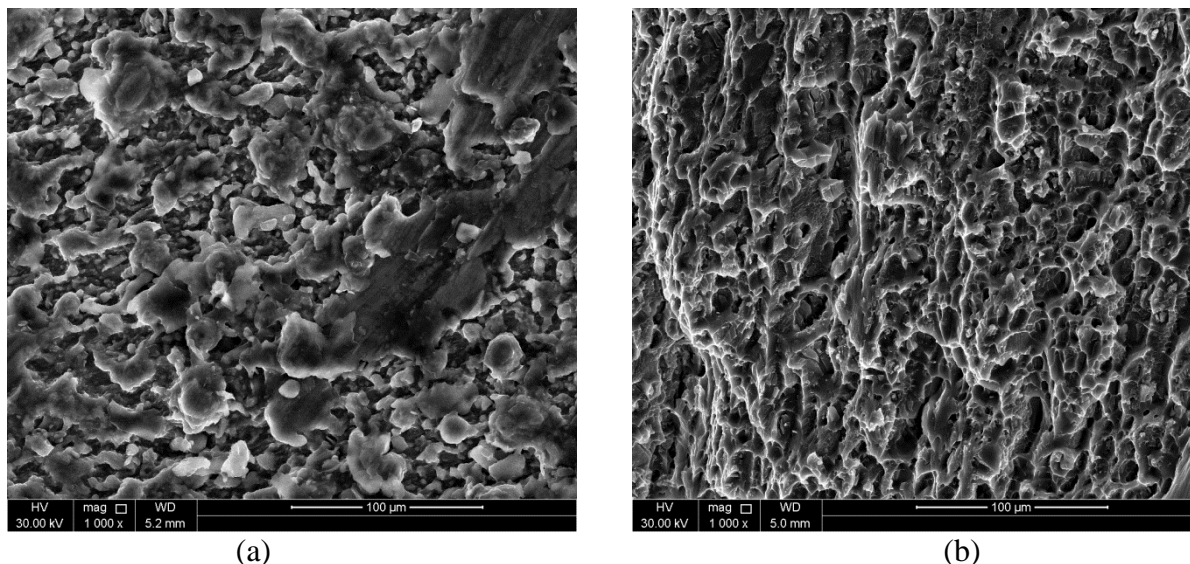


**Figure 12.** SEM micrographs of failed torsion specimens, (a) welded, (b) un-welded

## 5. CONCLUSIONS

This research investigated the effects of TIG welding on the corrosion and mechanical properties of Al alloy 6061 T6. The findings made by the experimental examination of welded and un-welded specimens can be given in the following:

- (1) The heat affected zone is more susceptible to corrosion than the rest of the base metal due to thermal alteration that resulted from the welding process.
- (2) The corrosion potential of the HAZ has fluctuated and it was more negative than the potential of the BM
- (3) TIG welding caused weakness on specimens that tested for tensile and torsion
- (4) The ultimate tensile strength of the TIG welded AA 6061 T6 specimens was 193.107 MPa which is 54% that of the base metal
- (5) The HAZ had the lowest hardness value.
- (6) The size and the spacing between the grains close to welded area were bigger compared to that located away from the weld.

## ACKNOWLEDGEMENT

This paper was made possible by NPRP grant No. 09-211-2-089 from Qatar National Research Fund (a member of Qatar foundation). The statements made herein are solely the responsibility of the authors.

## References

1. A. Hamdy, A. Beccaria, T. Temtchenko, *Surface and Coatings Technology*. 155 (2002) 176
2. S. Maggiolino, C. Schmid, *Journal of Materials Processing Technology*. 197 (2008) 237

3. Z. Nikseresht, F. Karimzadeh, M.A. Golozar, M. Heidarbeigy, *Materials and Design*. 31(2010) 2643
4. A. Squillace, A. De Fenzo, G. Giorleo, F. Bellucci, *Journal of Materials Processing Technology*. 152 (2004) 97
5. H.B Cary, *Modern welding Technology*. Prentice-Hall, NJ (1989)
6. ASM Specialty handbook: Aluminium and Aluminium alloys. ASM International Materials Park, Ohio (1994)
7. S. Kou, Y. Le, *Weld Journal*. 65 (4) (1986) 65
8. C.F. Tseng, W.F. Savage. *Weld Journal*. 50 issue 11 (1971) 777
9. G.M. Reddy, A.A. Gokhale, K. P. Rao, *J. Mater. Sci.* 32 (1997) 4117
10. M. Trueba, S.P. Trasatti, *Mater. Chem. Phys.* 121 (2010) 523
11. Z. S. Smialowska, *Corr. Sci.* 41 (1999) 1742.
12. X. Wl, Y. Tm, M. Hc. *J. Mater. Sci.*, 43 (2008) 942
13. W. Osorio, C. Freire, A. Garcia. *J Alloys Compd*, 397(2005) 179
14. C.G Rhodes, M.W. Mahoney, W.H. Bingel, R.A. Spurling, C.C. Bampton, *Scripta Materilia*. 36 (1997) 69
15. A. Cabello, G. Ruckert, B. Huneau, X. Sauvage, S. Marya. *J of Materials Processing Technology* 197(2008) 337
16. A. Kosstrivas, J.C. Lippold. *Welding journal*, 79 issue 1(2000) 1
17. H. Liu, H. Gu, Z. Wu, S. Leng, C. Yan, L. Zhang. *Trans. Nonferrous Met. Soc. China*. 21(2011) 477
18. B. Hu, I. M. Richardson. *J. Mater. Sci Eng.* 459 (2007) 94
19. S. Rajakumar, V. Balasubramanian. *Materilas and Design*.40 (2012) 17
20. Y.J Kwon, I. Shigematsub, N. Satio. *Materials Letters*. 62 (2008) 3827
21. N.H Tai, C.H. Yu. *J of Polymer Research*. 5, issue 3 (1998) 143
22. J.M. Hausmann, C. Leyens, W.A. Kaysser. *J. Mater Sci.* 39 issue 2 (2004) 501
23. M. Olsson, A.E Giannakopoul, S. Suressh. *J of Mechanics Physical Solids*. 43 issue 10 (1995) 1639
24. C. Menzemer, P.C. Lam, T.S Srivatsan, C.F Wittel. *Materials Letters* 41 (1999) 192